Optical techniques for direct imaging of exoplanets/Techniques optiques pour l'imagerie directe des exoplanètes

The Fourier–Kelvin Stellar Interferometer (FKSI)—A practical infrared space interferometer on the path to the discovery and characterization of Earth-like planets around nearby stars

William C. Danchi [a],*, Bruno Lopez [b]

[a] *NASA Goddard Space Flight Center, Exoplanets and Stellar Astrophysics, Code 667, Greenbelt, MD 20771, USA*
[b] *Observatoire de la Côte d'Azur, UMR 6203, BP 4229, 06304 Nice cedex 4, France*

Abstract

During the last few years, considerable effort has been directed towards large-scale (>\$1 billion USD) missions to detect and characterize Earth-like planets around nearby stars, such as the Terrestrial Planet Finder Interferometer (TPF-I) and Darwin missions. However, technological issues such as formation flying, cryocooling, null depth for broadband signals, control of systematic noise sources, budgetary pressures, and shifting science priorities at NASA and ESA, will prevent these missions from entering Phase A until the middle of the next decade. A simplified nulling interferometer operating in the near- to mid-infrared (e.g. ~3–8 microns), like the Fourier–Kelvin Stellar Interferometer (FKSI), can characterize the atmospheres of a large sample of the known planets. Many other scientific problems can be addressed with a system like FKSI, including the imaging of debris disks, active galactic nuclei, and low mass companions around nearby stars. We discuss the rationale, both scientific and technological, for a competed mission in the \$450–600 million (USD) range, of which FKSI is an example. *To cite this article: W.C. Danchi, B. Lopez, C. R. Physique 8 (2007).*
© 2007 Académie des sciences. Published by Elsevier Masson SAS. All rights reserved.

Résumé

FKSI, le 'Fourier–Kelvin Stellar Interferometer'—Un interféromètre spatial sur le chemin de la découverte et de la caractérisation des planètes de type Terre. Durant les dernières années, un effort considérable a été produit dans l'objectif de missions importantes telles que Darwin et TPF-I (Terrestrial Planet Finder Interferometer) pour la détection de planètes de type Terre autour des étoiles proches. Cependant, certains aspects technologiques critiques tels que le vol en formation, le refroidissement cryogénique, le taux de réjection sur une large bande passante en longueur d'ondes ainsi que le contrôle des sources d'erreurs systématiques rendent improbables les études de Phase A avant la fin de cette décennie. Un interféromètre simplifié comme le 'Fourier–Kelvin Stellar Interferometer', opérant dans l'infrarouge proche et moyen (de 3 à 8 microns), permet de caractériser un échantillon important des planètes extrasolaires déjà détectées par méthodes indirectes. Plusieurs autres sujets astrophysiques phares peuvent aussi être abordés par FKSI comme l'étude des disques de débris. Nous discutons dans cet article du fondement d'une mission de type 'mission moyenne' dont le coût s'échelonne entre \$450–600 million (USD), mission pour laquelle FKSI se positionne. *Pour citer cet article : W.C. Danchi, B. Lopez, C. R. Physique 8 (2007).*
© 2007 Académie des sciences. Published by Elsevier Masson SAS. All rights reserved.

* Corresponding author.
  E-mail addresses: wdanchi@milkyway.gsfc.nasa.gov (W.C. Danchi), lopez@obs-nice.fr (B. Lopez).

1. Introduction

Over the course of the last 10 years, more than 215 extra solar planets have been discovered (as of 15 March 2007) using a variety of observational methods, including precision radial velocity techniques [1,2], transit searches [3,4], microlensing [5,6], imaging [7], and pulsar timing [8]. A summary of data on all known exoplanets is maintained on J. Schneider's excellent website [9]. Of the 215 presently known planets, the vast majority of them (>181) were discovered using the radial velocity (RV) technique, and as the technique has improved from a precision of 3 m s^{-1} from a few years ago, to about 1 m s^{-1} currently. The lower limit of detectable masses has gone from around a Saturn mass (0.3 M$_J$) to Neptune (0.054 M$_J$) or Uranus (0.046 M$_J$) masses and to nearly Earth mass (0.017 M$_J$, Beaulieu et al. [6]). Fig. 1(a) displays a summary of the numbers of exoplanets and planetary systems discovered with each technique as of June 2006.

The long term focus of planet finding efforts at NASA are on the search for extrasolar terrestrial planets, like those within our own solar system, Venus, Earth, and Mars, and in particular, Earth-like planets within the habitable zone around stars similar to our own Sun, e.g., F, G, and K main sequence stars. At the present time, budgetary considerations and shifting science priorities within NASA have put the Terrestrial Planet Finder Interferometer (TPF-I) mission beyond the foreseeable future. Furthermore, the future course of the Darwin mission awaits the results of the upcoming ESA "Cosmic Vision 2015–2025" proposal cycle. However, even though the ultimate planet finding mission is not likely to happen for more than 15 years, it is important to realize that the planet finding community has many opportunities to move the field forward. Fortunately for both TPF-I and Darwin, significant progress has been made in the past few years in terms of formulating common science requirements and a common architecture for both missions. This progress was enabled by a letter of agreement between NASA and ESA that allowed shared membership between the Darwin and TPF-I science teams. This letter of agreement expired recently, but it is hoped that a new agreement will be forthcoming when needed.

However, a great deal of progress can still be made in the near term with missions under development that are significantly less expensive than the multi-billion dollar flagship missions. Indeed for the past five years, a group led by Danchi (PI) has developed a mission concept for the characterization of existing extrasolar planets, such as those discovered by the radial velocity technique (see for example, Danchi et al. [9,10], Barry et al. [11]). This mission concept, called the Fourier–Kelvin Stellar Interferometer (FKSI), is a near- to mid-infrared nulling and imaging inter-

Radial Velocity	155	Planetary systems
	181	Planets
	19	Multiple planet systems
Microlensing	4	Planets
Imaging	4	Planets
Pulsar Planets	2	Planetary systems
	4	Planets
	1	Multiple planet system
TOTAL	193	
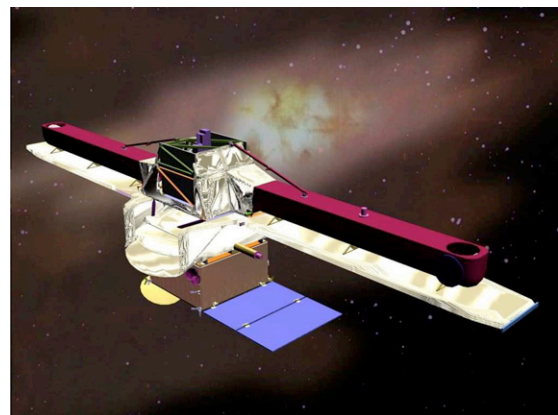
(a)   (b)

Fig. 1. (a) (Left panel) Summary of known exoplanets and techniques used for their discovery, as of June 2006. (b) (Right panel) Right panel is an artistic rendering of the Fourier–Kelvin Stellar Interferometer (FKSI) in space. It is a structurally connected interferometer with two 0.5 m-diameter telescopes on a 12.5 m boom, operating at 60 K, and with a wavelength range from 3–8 μm. It employs nulling and imaging interferometry and has a spectral resolution of about 25.
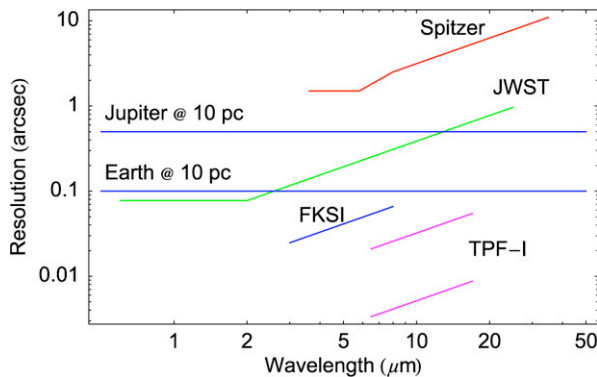
Orbital Parameters	What FKSI does:
Removes sin(I) ambiguity	Measure
Planet Characteristics	
Temperature	Measure
Temperature variability due to distance changes	Measure
Planet radius	Measure
Planet mass	Estimate
Planet albedo	Cooperative
Surface gravity	Cooperative
Atmospheric and surface composition	Measure
Time variability of composition	Measure
Presence of water	Measure
Solar System Characteristics	
Influence of other planets, orbit coplanarity	Estimate
Comets, asteriods, zodiacal dust	Measure

(a)   (b)

Fig. 2. (a) Left panel displays resolution in arcsec as a function of wavelength in microns. In the plot are current and proposed NASA infrared missions, including Spitzer, JWST, and TPF-I. Note that the FKSI mission occupies a unique space in terms of resolution and wavelength, having greater resolution than JWST, as well as better starlight suppression abilities and far greater resolution than Spitzer. It stands as a viable pathfinder mission for TPF-I as it employs the nulling interferometry technique and will be used to characterize the atmospheres of extrasolar planets. (b) Right panel. Summary of planet and solar system characteristics that can be measured or estimated from the FKSI mission.

feromter comprised of two 0.5 m diameter telescopes operating from 3 to 8 μm with a 12.5 m baseline on a boom, and passively cooled to about 60 K, as can be seen in Fig. 1(b). The designs for FKSI are well advanced beyond what is normally done in pre-phase A and the project has been focused on testbed activities for the past couple of years (e.g., see Barry et al. [12,13] and Frey et al. [14]). Detailed cost estimates have been made and a mission like the FKSI could easily fit into an Origins Probe scale budget ($600 million USD) or New Horizons budget ($750 million USD). In this article we will discuss some of the most important characteristics of the known exoplanets in Section 2. In Section 3 we review current studies of debris disks and discuss the unique discovery space available to a mission such as FKSI. We review the signal levels and noise sources involved in the detection of an interferometer. We show that the 3–8 μm region of the spectrum is very favorable for characterizing extrasolar giant planets (Figs. 2(b), 4) and a small interferometer is capable of detecting and characterizing them (Section 4). In Section 5 we discuss the status of the FKSI mission concept and related concepts such as Pegase.

2. Some characteristics of extrasolar planets

The currently known planets cover an impressively broad range of semi-major axes from about 0.02 AU up to about 6 AU and masses from about 10 M_J to about 0.02 M_J. These planets also cover a very wide range of eccentricities, which are quite different and distinct from our own Solar System. Interestingly, the bulk of known exoplanets have far larger eccentricities than planets in our Solar System, except for Mercury (0.21) and Pluto (0.25). Mars (0.093), Jupiter (0.048), Saturn (0.055), and Uranus (0.046) all have modest eccentricities, while the Earth and Venus have very low eccentricities, 0.016, and 0.006, respectively.

The origin of the close-in hot Jupiter like planets with very short periods is being actively investigated by Gaudi et al. [15] as is the much larger than anticipated eccentricity distribution. Such large eccentricities do not bode well for life in the sense that any organism would have to live through wide temperature variations that would occur between periastron and apastron, for example, such planets could be crossing the ice line in the more distant parts of their orbits. Of the 215 planets, 14 are transiting planets, and for these much more physical knowledge can be gained since the inclination angle (i), the planet radius (R_P) and hence the mean density can be determined. Spectroscopy can be used with the transiting planets to determine the temperature of the atmosphere (Deming et al. [16,17], Charbonneau et al. [18]), chemistry (Charbonneau et al. [19], Vidjal-Madjar [20]), and albedo (Rowe et al. [21]).

The frequency of extrasolar planets increases rapidly as the mass decreases with an approximately $1/M$ distribution. The lower limit on the detected mass of the planets is a result of the experimental techniques involved and many more planets are expected to be discovered in the next few years. The current pace of detected planets is of the order
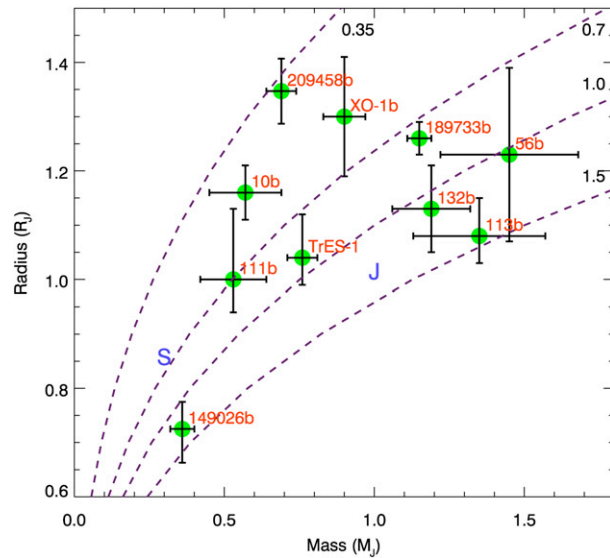
Fig. 3. Measured planet radius scaled to the radius of Jupiter as a function of mass scaled to a Jupiter mass for the ten transiting planets. Several curves are plotted for the radius as a function of planet mass for different mean densities indicated on the upper right side of the plot. The symbols S and J are plotted for Saturn's and Jupiter's parameters, respectively. Note most of the planets lie near the density of water, $\sim 1 \, \mathrm{g \, cm^{-3}}$. None of the transiting planets is considered rocky, for example, the mean density of the Earth $\sim 5 \, \mathrm{g \, cm^{-3}}$.

of about 30 per year. The mass distribution of the parent stars of the extrasolar planets is peaked at about 1.1 $\mathrm{M_\odot}$, which is not surprising since it is reflective of the stars in the solar neighborhood. Most of the stars are thus G and F stars, with a tail on the high mass end of a few A stars, and on the low mass end extending to a few K and M stars. Of course there are many low mass K and M stars within 30 pc of the Sun and the fact that very few planets have been discovered around such stars is mostly a product of the detection technique, in part because these stars have such low luminosities as well as more stellar activity than a normal F or G star. Not surprisingly, the distribution of distances of the currently known extrasolar planets peaks around 30–40 pc, with a tail extending to more than 100 pc. This distribution, while not indicative of any profound astrophysics, is interesting, nonetheless, because the angular resolution required to resolve the planet from the star is in a range that is amenable to modestly sized interferometers in the near-infrared, such as the FKSI system.

As mentioned previously, transiting planets have been extraordinarily useful in terms of expanding and deepening our knowledge of the physical parameters of extrasolar planets. By careful analysis of transit light curves it is possible to fit the planet radius and inclination angle to a fairly high precision, allowing a measurement of the mean density of the planets. Fig. 3 depicts measured planet radii scaled to the radius of Jupiter as a function of mass scaled to a Jupiter mass for the ten transiting planets. Several curves are plotted for the radius as a function of planet mass for different mean densities indicated on the upper right side of the plot. The symbols S and J are plotted for Saturn's and Jupiter's parameters, respectively. Note most of the planets lie near the density of water, which $\sim 1 \, \mathrm{g \, cm^{-3}}$. None of the transiting planets is considered rocky, for example, the mean density of the Earth is $\sim 5 \, \mathrm{g \, cm^{-3}}$, which has a much greater density than water.

The angular scale needed to resolve the planet from the star is determined from the semi-major axis length in AU when it is scaled by the distance, and this can be used to determine the required resolution of an imaging system, whether it be an interferometer or a filled-aperture telescope. For example, the nominal resolution $\lambda/(2B)$ of a space interferometer with baseline, B, at a center wavelength, λ, of 5 µm, is approximately 0.04 arcsec. A reasonable number of planets have semi-major axes with apparent separations greater than this angular size, but a more detailed analysis by Danchi et al. [10] demonstrates that it is possible to detect and characterize planets with semi-major axes much smaller than this. Clearly, a large number of extrasolar planets are, in principle, detectable with a space interferometer having a baseline of order ten meters. Detailed simulations, like those presented in Danchi et al. [10] have been performed and will be presented in a later publication. As of two years ago, we determined that at least 25 extrasolar planets can be detected and characterized with the FKSI system, and as detectors improve and more planets are discovered,
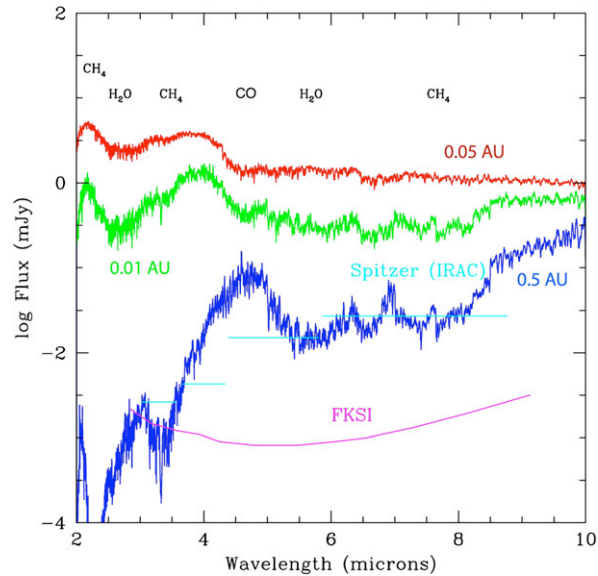
Fig. 4. Theoretical spectra for extrasolar giant planets at various distances from there host star (Seager [23]). Also plotted are sensitivity curves for the IRAC instrument on the Spitzer Space Telescope and the FKSI mission.

this number continues to increase. A detailed analysis will be published elsewhere. In the next section we review signal and noise sources that affect the detectability of extrasolar planets in the 3–8 μm, near-infrared to mid-infrared band.

Many molecular species, such as carbon monoxide, methane, and water vapor, might have strong spectral features in the 3–8 μm region, as can be seen in Fig. 4, which displays one example of model atmospheres for extrasolar planets calculated by Seager [23], for planets at various distances from the host star. Several parameters/hypothesis enter in such models: the range of temperature, the metallicities and cloud structures. The presence of clouds produces more 'flat' spectra (Marley et al. [24]). Identifying spectral features is a significant issue for future instruments. The red curve of Fig. 4 shows the theoretical spectrum of a very hot, close-in planet at 0.05 AU, while the blue curve displays spectrum for a much cooler planet ten times further out, at 0.5 AU. Also displayed are sensitivity curves for the IRAC instrument on Spitzer (light blue) and FKSI (purple). Clearly FKSI has sufficient sensitivity to detect a broad range of extrasolar planets.

3. Debris disks

3.1. Recent progress on debris disks

During the past few years, observers using the Spitzer Space Telescope and the James Clerk Maxwell Telescope have made progress on studies of the frequency of debris disks around solar type stars, and the characteristics of debris disks previously discovered by IRAS (Auman et al. [25], Plets and Vynckier [26]) and ISO (Spangler et al. [27]). The major focus of such studies has been on the decay of planetary debris disks (e.g., Rieke et al. [28]) and on the frequency of such disks around solar type stars (Bryden et al. [29], Beichman et al. [30], Kim et al. [31]). Debris disks have been discovered around stars having a range of masses, such as from A to K stars (e.g. Beichman et al. [30]), and white dwarf stars as well (Reach et al. [32]).

The lifetimes of debris disks of a large sample of A stars (masses around 2.5 $M_\odot$) have been shown to be ∼150 million years or less, with a substantial population of stars much older than that, with excesses, presumably caused by relatively recent episodes of collisions of large planetesimals (Rieke et al. [28]). The Spitzer MIPS observations at 70 μm of Beichman et al. [30] found that there were 6 of 26 main sequence stars (with RV known planets) with substantial debris disks, and hence that excess emission was as common around the main sequence stars as earlier observations of A and F stars with IRAS. Another important thrust of research on debris disks with Spitzer has been to push down the detection threshold as measured by L_{dust}/L_{star}, from about 10^{-3} with IRAS to as low as about 10^{-5}, as has been done by Kim et al. [31] using Spitzer. The morphology of debris disks has also been investigated

around a number of A stars, including ϵ Eri, β Pic, Fomalhaut, and Vega (Holland et al. [33,34]) at 450 and 850 μm, and HR 4796A (Koerner et al. [35], Jayawardhana et al. [36]) at 10 and 20 μm. These observations show a number of complex features, such as cavities, asymmetries, and clumps, which could be due to the resonant trapping of dust associated with a large planet, and other important dynamical phenomena such as collisional cascades of dust from interactions between planetesimals, and the interplay with effects like radiation pressure and Poynting–Robertson and gas collisional drag. These studies have focused on the cold outer regions of the debris disk systems, where the dust temperatures are around 50 K, which is a different population of dust than is most important for the search for earth-like planets in the habitable zone, where the dust should be around 300 K. Present limits are several orders of magnitude greater than expected for the hotter material in our own zodiacal cloud (Dermott et al. [37]), estimated to be $L_{dust}/L_{star} \sim 10^{-7}$–$10^{-8}$. Cooler material in our Kuiper belts is predicted to give $L_{dust}/L_{star} \sim 10^{-6}$–$10^{-7}$ (Stern [38]).

3.2. Disk parameter space to be explored with the FKSI system

Although a great deal of progress has been made in recent years on debris disks, a variety of instrumental limitations will prevent the community from achieving the progress that we need for the TPF-I and Darwin missions. There are two types of limitations. For Spitzer observations and likewise for Herschel and JWST, the main problem is that dust excesses are measured relative to the stellar spectrum, which is extrapolated to the infrared and compared with the observations. Calibration uncertainties limit the excesses measured to a few percent above the estimated stellar spectrum. This gives the limit from Spitzer of about 1000–1500 Solar System Zodis (SSZs). Another problem with the current observations is that they are most sensitive at the longer wavelengths, namely, 70 μm for Spitzer and at submillimeter wavelengths for the SCUBA observations at JCMT. Thus present observations constrain extrasolar zodiacal emission from the population of cool dust associated with distances of 10 AU and greater, which may have very different characteristics than the population of warm dust at 1 AU near the habitable zone, of most interest to TPF-I and Darwin. Ground-based nulling interferometers such as the Keck Interferometer Nuller and the nulling instrument on the Large Binocular Telescope Interferometer (LBTI), will make significant progress on this latter population of dust since they will observe at 10 μm near the peak of the 300 K blackbody emission. However, our present understanding of the limitations of ground-based warm nulling systems is that they will push the limit to about 100–150 SSZs around nearby stars, still far larger than is needed for sizing the TPF-I and Darwin missions. The reason ground based nulling interferometers can make such significant progress is that they suppress the star light and enable a clearer distinction between stellar and zodiacal light, thus bypassing the limitations of a purely spectroscopic approach. Another limitation to present studies is the lack of spatial resolution. This is especially significant as clumps and asymmetries in the distribution of debris disk material can be used to search for unseen planets. Furthermore, it is vitally important to know that the emission is coming from the region of the habitable zone, and to know the amount of dust for the TPF target stars. It is unlikely that we can know for certain what are the best TPF target stars (from the standpoint of exozodiacal dust) without such a mission. As a comparison, coronagraphic observations on JWST have an inner working angle (IWA) of $\sim 4\lambda/D \sim 0.7$ arcsec at $\lambda = 5$ μm and $D = 6$ m. This IWA can be compared with the Solar System viewed at 10 pc, where the Earth at 1 AU is at an angular radius of 0.1 arcsec. Thus, this much larger IWA means that JWST will not be able to probe the dust and planets in the region near the habitable zone for nearby stars, only zones corresponding to the outer planets and Kuiper belts.

4. Understanding signal-to-noise ratios for a rotating nulling Bracewell interferometer

We turn now to some recent calculations of signal and noise sources affecting the detection and characterization of exoplanets in the 3–8 μm region of the spectrum. Fig. 5(a) displays a calculation of the expected signal levels in Jy (10^{-26} W m^{-2} Hz^{-1}) as a function of wavelength (μm) for our Sun and planets in our solar system if it were viewed from a reference distance of 10 pc. We also display flux density levels for extrasolar giant planets at 400 K and 1000 K, for an exoplanet with radius ($1.35R_J$) and albedo of HD209458b. The radii and albedos of the solar system planets were taken from the tables from Lissauer and DePater [22]. It is clear from the plot that the amount of starlight suppression needed to detect an extrasolar giant planets is of the order of 10^{-4} and also that the Earth itself will be very difficult to detect as its expected signal level is 0.3 μJy at 10 μm. Venus emits less at 10 μm than the Earth despite its high surface temperature (several hundred K) because what is seen at 10 μm is the temperature
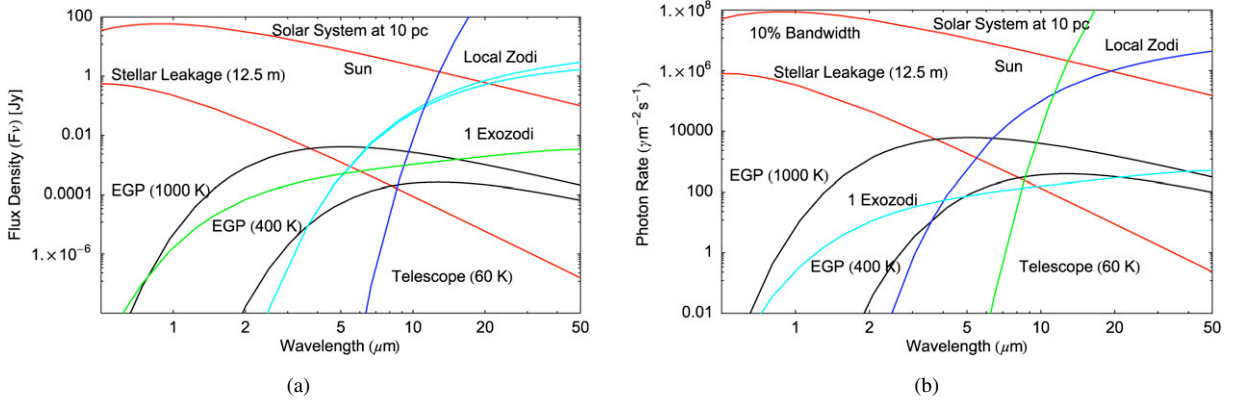
Fig. 5. (a) Left panel displays a calculation of the expected signal levels in Jy (10^{-26} W m^{-2} Hz^{-1}) as a function of wavelength (μm) for our Sun and planets in our solar system if it were viewed from a reference distance of 10 pc. We also display flux density levels for extrasolar giant planets at 400 and 1000 K, for an exoplanet with radius ($1.35 R_J$) and albedo of HD209458b. The radii and albedos of the solar system planets were taken from the tables from Lissauer and DePater [22]. (b) Right panel is based on (a) in which we have calculated the rate in photons m^{-2} s^{-1} assuming a 10% bandwidth.
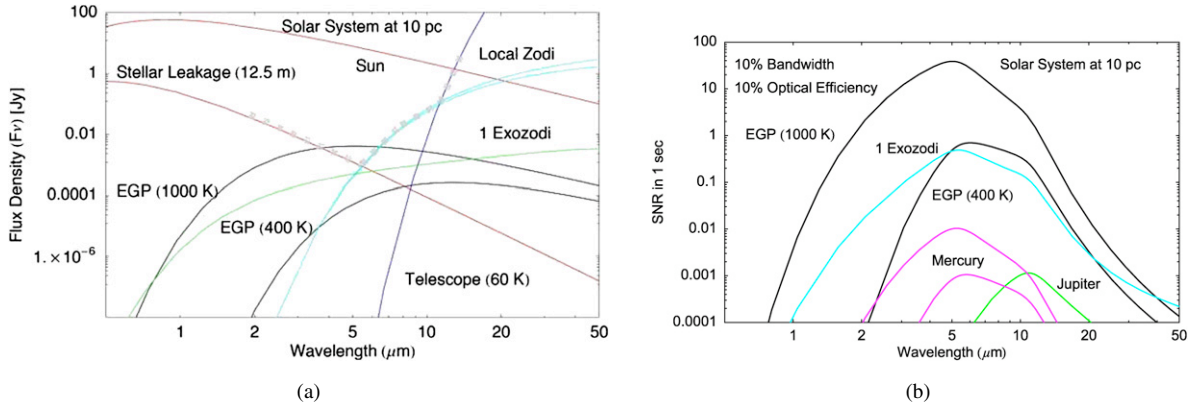

Fig. 6. (a) Left panel displays expected noise sources that affect the detection and characterization of exoplanets using a nulling interferometer including stellar leakage (due to the finite size of the star), the exozodiacal signal (based on the model discussed in Reach et al. [39]) from a exozodiacal cloud having the same characteristics as our own zodiacal cloud, the local zodiacal cloud itself, and the thermal emission from the telescope mirrors, assumed to be cooled to 60 K. (b) Right panel shows the expected signal to noise ratio in 1 s for a 1 m^2 mirror, assuming a 10% bandwidth, and 10% optical efficiency.

of the clouds, which are significantly cooler than the surface. Using the curves in Fig. 5(a) we have calculated the rate in photons m^{-2} s^{-1} assuming a 10% bandwidth. The result is shown in Fig. 5(b). From this figure it is clear that the photon rate from a hot or warm Jupiter is hundreds or thousands of photons m^{-2} s^{-1} whereas the photon rate from an Earth-like planet is less than one photon m^{-2} s^{-1}. This is a fundamental reason why it is so much easier to detect and characterize the giant exoplanets than Earth-like planets. Clearly, for the former case, we can make significant progress with relatively small apertures, assuming typical optical efficiencies, whereas in the latter case we will need apertures that are at least factors of ten greater, on the order of many m^2 instead only ~1 m^2. This is also a very significant cost driver for any space mission or ground-based system as well. Fig. 6(a) displays expected noise sources that affect the detection and characterization of exoplanets using a nulling interferometer including emission from the stellar leakage (due to the finite size of the star), emission from the exozodiacal dust cloud (based on the model of Reach et al. [39]) from a dust cloud having the same characteristics as our own zodiacal cloud, emission from the local zodiacal cloud itself, and the thermal emission from the telescope system, assumed to be cooled to 60 K. Also drawn is a gray dashed line that shows the boundary created by the dominant noise sources as a function of wavelength, from stellar leakage, which is most important at short wavelengths, to the emission from the local zodiacal cloud, which dominates at the middle wavelengths, and the emission from the telescope itself at the longest wavelengths. We see that the region from 3 to 8 or even 10 μm is very favorable from a signal to noise ratio standpoint. Fig. 6(b) shows

the expected signal to noise ratio in 1 s for a 1 m^2 mirror, assuming a 10% bandwidth, and 10% optical efficiency. Clearly the warm and hot exo-Jupiters are easy to detect with this short integration time as are exozodiacal clouds. Given longer integration times, small hot planets such as Mercury are detectable, as are cooler, large planets like Jupiter.

5. Instrument and mission design considerations

A specific implementation of a extrasolar planet characterization mission in the infrared is the FKSI mission concept discussed briefly at the beginning of this paper. This mission has been under development beginning five years ago by our group at Goddard Space Flight Center (GSFC) and many details of the design studies have been published in various SPIE proceedings and other publications (e.g., Danchi et al. [11,40], Hyde et al. [41], Barry et al. [12,13], and Frey et al. [14]). In this section we review some of the main aspects of the mission concept including goals, requirements flowdown, the status of some of the mission's testbed, and a comparison with other mission concepts and ground-based science and technology precursors.

5.1. Mission goals and uniqueness to NASA

The high spatial and spectroscopic resolving capability of the FKSI instrument (as shown in Figs. 4 and 6(b)) together with its calculated sensitivity will position it as an important facility for the study of a range of astronomical phenomena. Its science objectives are, very broadly, to directly detect extrasolar giant planets (EGP), study debris disks and the evolution of protostellar and evolved stellar systems, and to facilitate the study of extra-galactic star formation regions and the extended neighborhoods of active galactic nuclei. To answer key questions about these planets FKSI will be able, depending on configuration, to detect at least 25 known EGPs and make precise determination of their orbital parameters. The spatial resolution of the Fourier–Kelvin Stellar Interferometer together with the instrument's R ∼ 25 spectroscopic capability will allow the direct detection and analysis of photons from EGPs under certain conditions of orbital phase and angular separation. (See Danchi et. al. [40].) These measurements will enable studies of the environmental conditions to which the planet is subject. They will also provide a means of measuring the composition of the planet's atmosphere. FKSI exploits the orbital dynamics of close-in planets. Using a spatial dither of the null fringe, FKSI will be able to reconstruct the astrometric orbit of the planet and, in combination with radial velocity studies, derive the mass. In addition to mass, FKSI observes the variation in the planet's infrared spectrum as a function of phase, and facilitates characterization of the planet's thermal state and composition. In favorable cases, data obtained using FKSI could even allow scientists to make inferences about dynamical properties such as winds, e.g., Showman and Guillot [42] and Guillot and Showman [43]. This approach of exploiting the infrared brightness of close-in planets builds on the transit and radial velocity studies, which have detected most of the known extrasolar planets.

While direct detection of EGPs is a principal goal of the FKSI mission, study of stellar environments in general will also be greatly facilitated by the instrument's spatial and spectral resolving power. With FKSI, scientists may observe the formative stages of planetary systems, protoplanetary disk structure, the evolution of primordial exozodiacal dust, and debris disks about various stellar types. These observations may then be used to determine the characteristics of circumstellar material that could lead to planet formation or the evolution of the habitable zone about post-main sequence stars. These studies would facilitate refinement of the target lists and science goals of the TPF mission.

Fig. 2(a) places the FKSI mission in the overall context of current and future NASA infrared missions by plotting the angular resolution in arcsec as a function of wavelength in microns. In the plot are current and proposed NASA infrared missions, including Spitzer, JWST, and TPF-I. Note that the FKSI mission occupies a unique space in terms of resolution and wavelength, having greater resolution than JWST, as well as better starlight suppression abilities than expected for JWST coronagraphs and far greater resolution and better sensitivity than the Spitzer Space Telescope. It stands as a viable pathfinder mission for TPF-I as it employs the nulling interferometry technique and will be used to characterize the atmospheres of extrasolar planets. Indeed the measurement capabilities table presented in Fig. 2(b) is very similar to that of TPF-I as presented in the Navigator Program Science Plan currently under development.
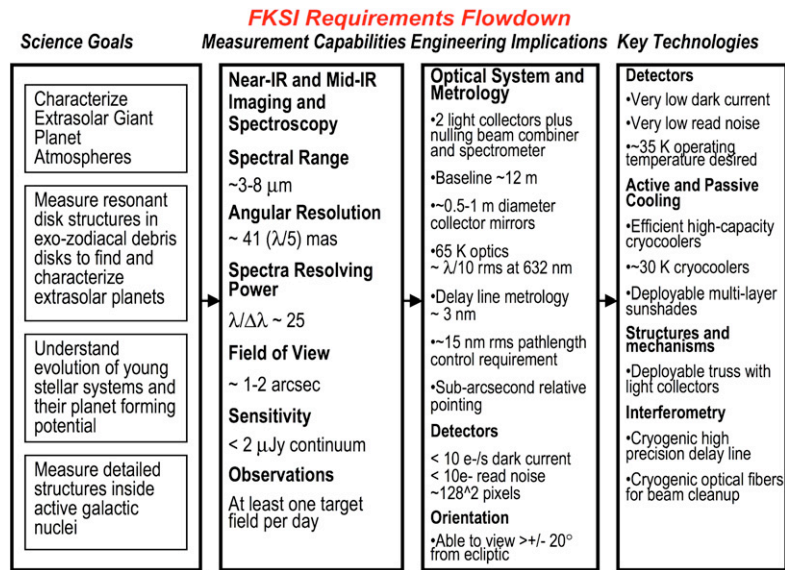
Fig. 7. FKSI requirements flowdown showing derivation of specific engineering requirements and key technologies and their relationship to mission science goals.

5.2. Brief review of the FKSI mission concept and related concepts

Our team consists of scientists from a broad array of institutions and, together, with engineering support from GSFC, has expended significant effort to develop a range of design options for FKSI. We have studied various beam combination techniques and array architectures in preparation for submission of FKSI as a Discovery-class mission. These design studies were conducted initially at GSFC's Instrument Synthesis and Analysis Laboratory and the Integrated Mission Design Center. These are important functions within GSFC's infrastructure used to facilitate rapid vetting of various mission and instrument design concepts. These studies were then augmented by the work of a larger, focused team of experienced scientists and engineers dedicated to the FKSI mission. The resulting design is a nulling interferometer configuration with an optical system consisting of two 0.5 to ∼1 m telescopes on a 12.5 to 20 m boom feeding a symmetric Mach–Zehnder beam combiner. A null tracker and hollow-core waveguide optical fiber for wavefront cleanup further augment the system and allow it to produce the required 0.01% null of the central starlight. The flowdown of requirements from science goals to key technologies is given in Fig. 7. The overall system block diagram is shown in Fig. 8(a) and discussed in detail in Barry et al. [13] and other publications.

Presently a similar concept called Pegase was developed by a team in France from a call for proposals from CNES for formation-flying space mission concepts. The Pegase mission concept was for a three spacecraft formation, with two spacecraft with ∼0.4 m flat mirrors reflecting starlight into a central beam combination facility and operating at ∼100 K in the 2–5 μm wavelength range (Duiguou et al. [44]). These mirror-satellites optically are identical to the flat mirrors on the ends of the FKSI booms. The Principal Investigators from the FKSI and Pegase teams have met, and it is possible to combine the missions, with the Pegase mirror-satellites deployed from the FKSI booms. The advantage of this architecture is that complete in-flight testing and science operations can take place as a structurally connected system, with formation-flying taking place afterwards. In this way science productivity can be maximized and risk minimized.

5.3. Ground-based science and technology developments

Two ground-based nulling interferometry technology and science projects are under development in the US. The further advanced is the Keck Interferometer Nuller (KIN) (Serabyn et al. [45]) which utilizes two nulling interferometers formed from separate halves of the 10 m Keck Telescopes. The separation between the two Keck Telescopes is 85 m. The nulled outputs of these two nullers are then combined on a beamsplitter. A complex chopping scheme is employed using this system to achieve two goals: (i) to null out the starlight; and (ii) to chop out the atmospheric and
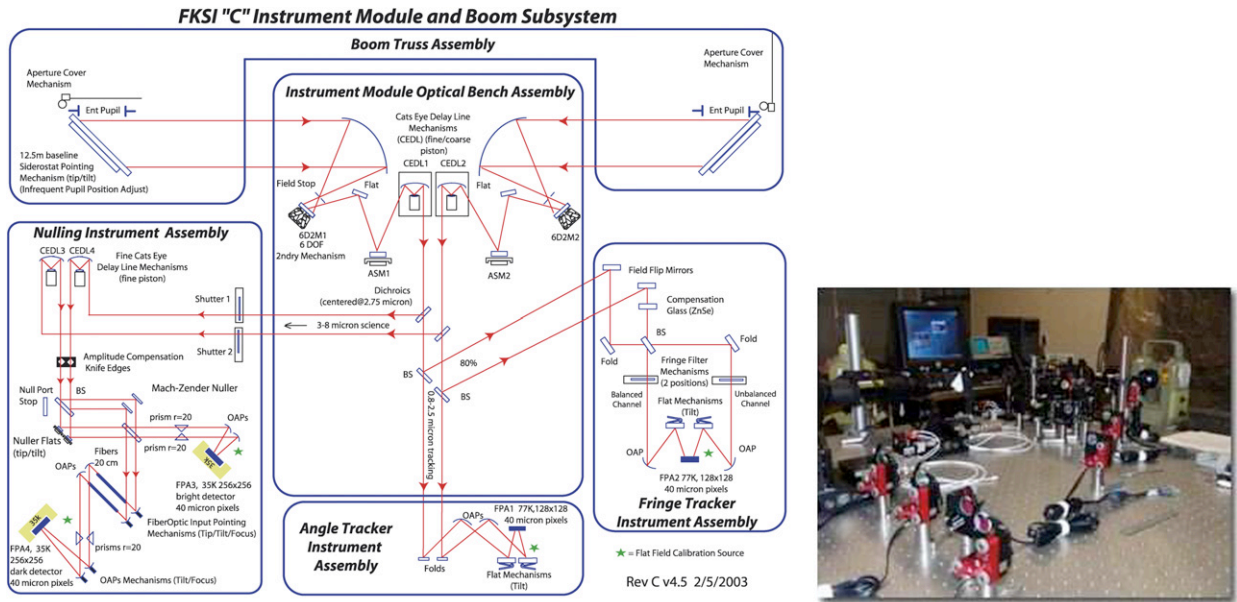
Fig. 8. (a) Left panel. Schematic of detection system for FKSI. (b) Right panel. FKSI nulling testbed in the Horizontal Flow Facility at Goddard Space Flight Center.

telescope emission, which is the principal source of noise at 10 μm in ground-based infrared observing. Considerable progress has been made with this system, and it is currently undergoing testing on the sky. Preliminary observations indicate that it is like to achieve a lower limit for extra-solar zodiacal emission from nearby stars, of the order of 100–150 solar system zodis at 10 μm (Colavita et al. [46]).

Another system developed in the US for nulling observations is the Large Binocular Telescope Interferometer (LBTI) (Hinz et al. [47]) that will combine the two 8 m telescopes of the LBT that are on an approximately 14 m baseline. This system employs the two 8 m telescopes that are fixed on a common altitude-azimuth (alt-az) mount. It is expected that this system will provide somewhat better sensitivity that the Keck Interferometer Nuller because it has an optical train with many fewer elements and hence greater transmission and lower emissivity. Hopefully the LBTI will be able to achieve somewhat lower limits for extra-solar zodiacal emission than the Keck Interferometer Nuller.

A third ground-based system under development is ALLADIN, which is a proposed two element nulling interferometer for operation at Antarctica's Dome C. Progress has been made on basic designs for this system, and work has been in progress to deal with the problem of the atmospheric turbulence near the ground, which is one of the principal limitations to the projected performance of this system. Designs are under consideration in which the telescopes and other system infrastructure will be supported on towers ∼30 m in height (Swain et al. [48]).

5.4. The FKSI testbeds and status

In order to reduce risk for the mission itself, the FKSI project undertook the development of two testbeds, as described in the papers by Barry et al. [12,13] and Frey et al. [14]. The first testbed is a model of the essential elements of the FKSI detection system, including the modified Mach–Zehnder beam combiner (the main element of the FKSI nuller assembly), and the optical fiber wavefront cleanup assembly, and detectors. This system is fed by a pseudo-star created by a laser or blackbody source coming through a pinhole to represent a point source. The light is further fed through two cats-eye delay lines in order to equalize the pathlengths from the source. A control system has been developed to model the actual control system anticipated in the flight hardware (Hyde et al. [27], Frey et al. [14]). A recent photo of the completed testbed is shown in Fig. 8(b). A second testbed was also developed to test out a dither-less quadrature phase detector that is proposed for part of the FKSI fine delay line control for the nuller portion of the detection system. This system has also been described in the papers cited above, particularly in the most recent papers by Barry et al. [12] and Frey et al. [14]. Within the next year we expect to achieve the desired results for the FKSI mission, which was a broadband null depth of better than 10^{-4}, which is sufficient for the mission

goals, as discussed in Danchi et al. [10,11]. This gives the project the desired maturity to be able to propose to the appropriate NASA mission category, for example, the Discovery program if done with a European partner, an Origins Probe program, if one is successfully created in the next few years, or the New Horizons program if it is broadened to allow proposals from groups working on extrasolar planet science.

6. Summary

We have presented the rationale and progress towards a mid-priced category mission ('Origins Probe' scale) to characterize the atmospheres of currently known extrasolar planets. We have described why the 3–8 µm region is particularly favorable from a signal-to-noise ratio standpoint, and that such a mission can be accomplished with a relatively simple, passively cooled (60 K) two-telescope space interferometer operating at L2. Such an interferometer only needs a collecting area of about 1 m^2 in order to be able to detect a large number of existing extrasolar planets with modest integration times. The practical realization of these ideas is the Fourier–Kelvin Stellar Interferometer (FKSI), which is at an advanced stage of preparation. Thus we have shown that even in a cost-constrained era, such as we face today, it is possible for our planet finding community to develop moderately priced space missions that can move our field forward.

Acknowledgements

References

[1] M. Mayor, D. Queloz, Nature 378 (1995) 55.
[2] G.W. Marcy, P. Butler, Annu. Rev. Astron. Astrophys. 36 (1998) 57.
[3] D. Charbonneau, et al., Astrophys. J. 529 (1999) 45.
[4] R. Alonso, et al., Astrophys. J. 613 (2004) L153.
[5] D.P. Bennett, et al., Nature 402 (1999) 57.
[6] J.-P. Beaulieu, et al., Nature 439 (2006) 437.
[7] G. Chauvin, et al., Astron. Astrophys. 438L (2005) 25.
[8] A. Wolszczan, D. Frail, Nature 355 (1992) 145.
[9] J. Schneider, http://euoplanets.eu, 2006.
[10] W.C. Danchi, et al., Astrophys. J. 597L (2003) 570.
[11] W.C. Danchi, et al., Proc. SPIE 5491 (2004) 236.
[12] R. Barry, et al., Proc. SPIE 6265 (2006), in press.
[13] R. Barry, et al., Proc. SPIE 5905 (2005) 311.
[14] B. Frey, et al., Proc. SPIE 6265 (2006), in press.
[15] B.S. Gaudi, et al., Astrophys. J. 628 (2005) 73.
[16] D. Deming, et al., Nature 434 (2005) 740.
[17] D. Deming, et al., Astrophys. J. 644 (2006) 560.
[18] D. Charbonneau, et al., Astrophys. J. 626 (2005) 523.
[19] D. Charbonneau, et al., Astrophys. J. 568 (2002) 377.
[20] A. Vidal-Madjar, et al., Nature 422 (2003) 143.
[21] J.P. Rowe, astro-ph/0603410, 2006.
[22] J. Lissauer, I. DePater, Planetary Sciences, Cambridge Univ. Press, Cambridge, UK, 2001.
[23] S. Seager, Private communication, 2005.
[24] M.S. Marley, et al., ProtoStars and Planets, vol. 5, 2007, p. 733.
[25] H.H. Aumann, et al., Astrophys. J. 278 (1984) L23.
[26] H. Plets, C. Vynckier, Astron. Astrophys. 343 (1999) 496.
[27] C. Spangler, et al., Astrophys. J. 555 (2001) 932.
[28] G.H. Reike, et al., Astrophys. J. 620 (2005) 1010.
[29] G. Bryden, et al., Astrophys. J. 636 (2006) 1098.
[30] C.A. Beichman, et al., Astrophys. J. 622 (2005) 1160.
[31] J.S. Kim, et al., Astrophys. J. 632 (2005) 659.
[32] W. Reach, et al., Astrophys. J. 635 (2005) L161.
[33] W. Holland, et al., Nature 392 (1998) 788.
[34] W. Holland, et al., Astrophys. J. 582 (2003) 1146.

[35] M. Koerner, et al., Astrophys. J. 503 (1998) L83.
[36] R. Jayawardhana, et al., Astrophys. J. 503 (1998) L79.
[37] W. Dermott, et al., Asteroids III, Univ. of Arizona Press, Tucson, 2002, p. 423.
[38] S.A. Stern, Astron. Astrophys. 310 (1996) 999.
[39] W. Reach, et al., Icarus 164 (2003) 384.
[40] W.C. Danchi, et al., Proc. Conf. on Towards Other Earths, ESA SP-539, ESA Publication Division, Nordwijk, Netherlands, 2003.
[41] T.T. Hyde, et al., Proc. SPIE 5497 (2004) 553.
[42] A.P. Showman, T. Guillot, Astron. Astrophys. 385 (2002) 166.
[43] T. Guillot, A.P. Showman, Astron. Astrophys. 385 (2002) 156.
[44] J.M. Le Duigou, et al., Proc. SPIE 6265 (2006).
[45] E. Serabyn, et al., Proc. SPIE 6268 (2006).
[46] M. Colavita, et al., Private communication, 2007.
[47] P. Hinz, et al., Proc. SPIE 6268 (2006).
[48] M. Swain, et al., Proc. SPIE 6268 (2006).